

# Clutch Chatter

Dipl.-Ing. Paul Maucher

One primary goal of automotive development is the elimination of torsional vibration and its associated noises in the motor vehicle drive train. One of the previous presentations cited various types of torsional vibrations and their excitation sources, including frictional vibration in the drive train and its source, "the chattering clutch."

These frictional vibrations, generally called clutch chatter, judder, or shudder, pose a problem that remains unsolved even today, although it has been around ever since the automobile was invented. Designers are still trying to eliminate or improve by the dubious and time-consuming "trial and error" method. The chatter problem has even been exacerbated by the shift from asbestos to non-asbestos facings and therefore urgently requires thorough, systematic investigation.

Consequently, the following discussion deals with torsional vibrations generated in the vehicle drive train by clutch chatter, its causes, and the basic principles governing this behavior. These studies are limited to dry friction clutches. However, the general insights established here apply in principle to wet friction clutches as well.

## Sources of Chatter Vibrations

Figure 1 shows a typical start-up. During clutch engagement, that is, during the slip phase, the transmission shaft is accelerated from an at-rest condition up to the engine speed. For start-up without chatter, the acceleration of the transmission shaft is very uniform, as shown by the broken line in the illustration. On the other hand, when chatter is involved during start-up, vibrations occur in the form of periodic torsional vibrations, which generally continue as a rule until the transmission has come up to engine speed. Chatter manifests itself as objectionable, oscillating vehicle acceleration in the form of surging and annoying vehicle noise.

The literature [1 – 3] contains only a few publications on the subject of frictional vibrations, and positions tend to be contradictory.

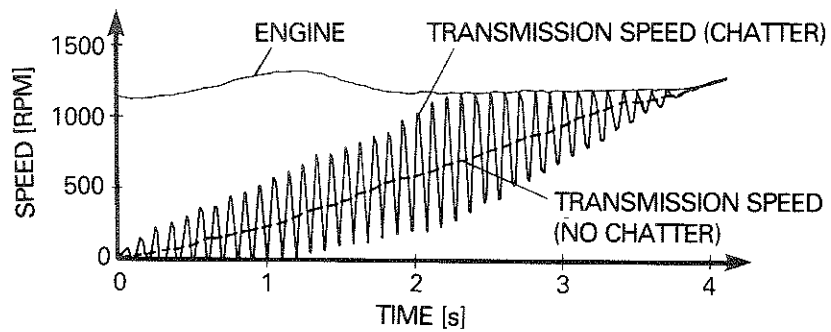


**Figure 1:** Start-up curves with and without chatter vibrations

Current thinking attributes chatter to a decreasing friction coefficient of the clutch facings, coupled with increasing slip speed. The following discussion characterizes this curve with a decreasing friction coefficient and negative gradients of the friction coefficient.

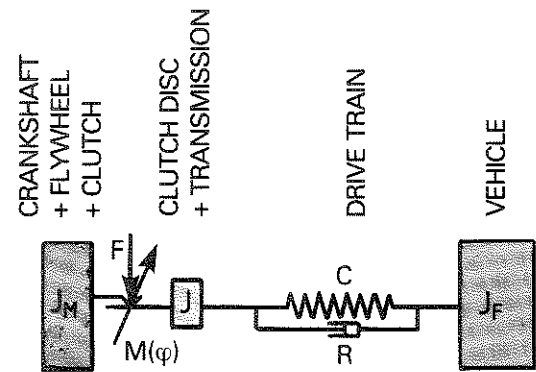
In addition to the previously cited decreasing friction coefficient, additional sources for chatter vibrations in motor vehicle drive trains include:

- the torsional irregularity of the engine
- clamp load fluctuations due to lack of parallelism between the clutch and the clutch disc
- inadequate drive train damping.

### **The Frictional Vibration Model for the Motor Vehicle Drive Train**

We have simplified the drive train vibration model in order to provide a graphic representation of the physical relationships involved in clutch chatter and its associated frictional vibrations (Figure 2). The clutch disc and the transmission are represented by the combined inertia  $J$ , which is connected to the vehicle inertia  $J_F$  by a spring and damper system. The inertia  $J_F$  is assumed to be  $\infty$  because it is very great in comparison to  $J$ . The inertia  $J_M$  for the crankshaft together with the flywheel and the clutch is also viewed as a very large and constantly rotating inertia.

## VIBRATION MODEL



$$\text{CLUTCH TORQUE } M(\varphi) = F \cdot 2 \cdot r \cdot \mu(\varphi)$$

**Figure 2:**

Simple vibration model of the drive train

RELATED DIFFERENTIAL EQUATION

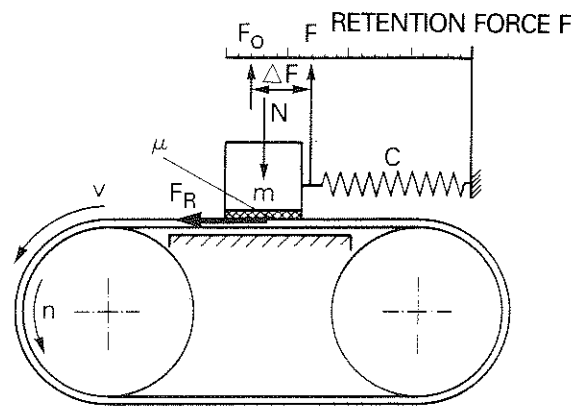
$$J \cdot \ddot{\varphi} + R \cdot \dot{\varphi} + C \cdot \varphi = M(\varphi) = F \cdot 2 \cdot r \cdot \mu(\varphi)$$

During start-up, the clutch disc creates a frictional connection with the engine via the clutch, being only partially closed. The frictional torque  $M$  of the clutch is established by the clamp load  $F$ .

### **Load Transmission due to Friction The Effect of the Decreasing Friction Coefficient on the Vibration System**

The friction facing, reflected by the curve of its friction coefficient, is the essential element involved in torque transmission. Fluctuations in the friction coefficient play no role in stationary force transmission, in contrast to engagement during vehicle start-up.

The model in Figure 3, which was already used in the previous presentation, is designed to explain the effect of the friction coefficient curve in a vibrating system.



MAXIMUM FRICTION FORCE  $F_{R0} = N \cdot \mu_0$

MINIMUM FRICTION FORCE  $F_R = N \cdot \mu$

$$\Delta F = F_0 - F = N (\mu_0 - \mu)$$

**Figure 3:**  
Effect of the decreasing friction coefficient in the vibration system

A body is pressed with normal force  $N$  against a moving belt driven by two rollers. The body is retained by an elastic spring.

We can make the following assumption with respect to the friction coefficient: the friction coefficient is at its greatest as static friction and decreases as the slip speed increases.

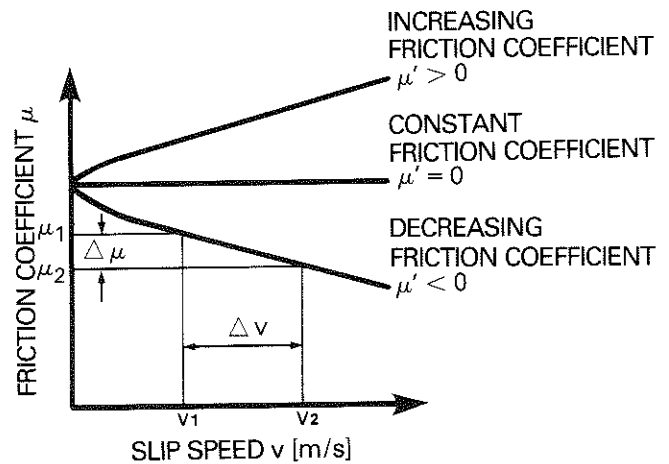
If the belt is driven at a constant speed, the body initially moves along with the belt, whereby the static friction force  $F_{R0}$  generated between the body and the belt deflects the spring. As soon as the retention force  $F_0$  reaches the maximum friction force  $F_{R0} = N \cdot \mu_0$ , the body stops moving. The belt continues to move, which results in relative movement between the body and the belt. The friction coefficient changes from the static to the lower dynamic friction coefficient. The friction force generated between the body and the belt is reduced by the fact that the body migrates back toward its original position. Its slip speed relative to the belt increases until a new equilibrium is established. The body stops moving, which again decreases the slip speed between the body and the belt. The friction coefficient, and hence the friction force, increases again, so that the body is once more carried along by the belt. The same process repeats itself, producing a periodic back-and-forth motion in the spring-anchored body. This motion is caused by the falling friction coefficient, which is itself attributable to the increasing slip speed. This is the explanation for self-induced frictional vibration.

## The Gradient of the Friction Coefficient

Testing and evaluation of facing materials with respect to chatter properties requires that we define a generally applicable identifying variable for the slip-speed-dependent friction coefficient curve (Figure 4). This slip-speed-dependent friction coefficient curve is defined as the gradient of the friction coefficient

$$\mu' = \frac{\Delta \mu}{\Delta v} = \frac{\mu_2 - \mu_1}{v_2 - v_1} \text{ [s/m]}.$$

and is used in the following calculations and discussions.



DEFINED AS THE GRADIENT OF THE FRICTION COEFFICIENT

**Figure 4:**

Gradient of the friction coefficient  $\mu'$

$$\mu' = \frac{\Delta \mu}{\Delta v} = \frac{\mu_2 - \mu_1}{v_2 - v_1} \text{ [s/m]}$$

If the friction coefficient increases with increasing slip speed, then  $\mu' > 0$  and the gradient of the friction coefficient is positive. If the friction coefficient decreases as the slip speed increases, then  $\mu' < 0$  and is negative. If the friction coefficient is constant with respect to the slip speed, then  $\mu' = 0$ , as described in Coulomb's law.

## Calculating Frictional Vibrations

The frictional vibration behavior of the simplified drive train as represented in Figure 2 is influenced by the following factors:

- the gradient of the friction coefficient  $\mu'$
- the damping value R
- the inertia J
- the drive train spring rate C
- the clamp load F for the slipping clutch.

The torsional vibrations for this vibration model are described by the differential equation

$$J \cdot \ddot{\varphi} + R \cdot \dot{\varphi} + C \cdot \varphi = M(\varphi)$$

where the clutch torque,  $M(\varphi) = F \cdot 2 \cdot r \cdot \mu(\varphi)$ , varies with the slip speed and acts as a vibration source.

All these calculations are based on a  $\varnothing$  200 clutch with a friction radius of  $r = 84.5$  mm.

Figure 5 shows simulation calculations for an engine speed of 1000 rpm, an output speed of 750 rpm and a clamp load of 1500 N.

The damping value and the gradient of the friction coefficient were varied in the form of a matrix. From the top to the bottom, the gradient of the friction coefficient decreases from 0 to  $-15 \cdot 10^{-3}$  s/m. From left to right, the damping value increases from 0.005 to 0.3 Nms. Each individual graph in the matrix shows the speed vibration of the clutch disc as a function of time. There are virtually no or very minimal vibrations for  $\mu' = 0$ , regardless of damping. These vibrations increase as the gradient of the friction coefficient decreases, but decrease with increased damping. They disappear beyond a certain damping value, which is greater the lower the gradient of the friction coefficient.

Let us assume that  $\mu'$  is constant with respect to the slip speed, that is, that the friction coefficient decreases linearly with respect to the slip speed. We can then use the differential equation to derive the limiting condition for the incidence of frictional vibrations

$$R = -2 \cdot F \cdot r^2 \cdot \mu'$$

If the damping value  $R > -2 \cdot F \cdot r^2 \cdot \mu'$ , the system is vibration-free.

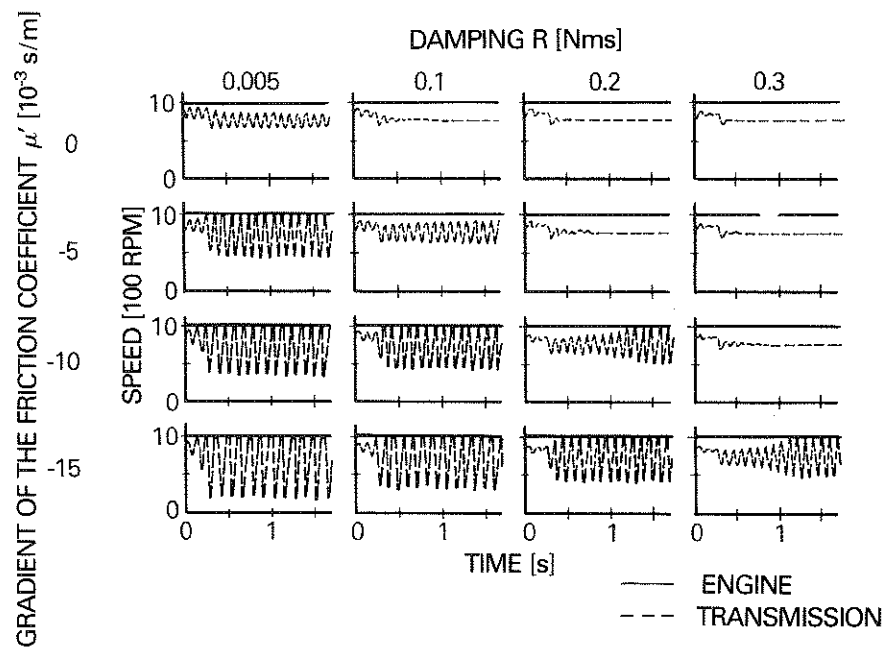


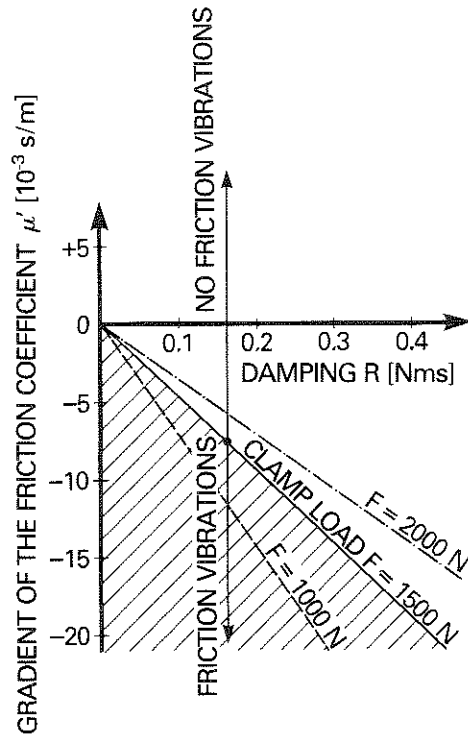
**Figure 5:** Torsional vibrations as a function of damping and of the gradient of the friction coefficient

On the other hand, if  $R < -2 \cdot F \cdot r^2 \cdot \mu'$ , frictional vibration occurs. The greater the currently prevalent clamp load  $F$ , the greater the damping value required to prevent frictional vibrations. The graph in Figure 6 shows this limiting condition plotted as a function of the damping value and the gradient of the friction coefficient. The lines plotted on the graph represent different values for  $R = -2 \cdot F \cdot r^2 \cdot \mu'$ , where the clamp load  $F = 1000$  N is represented as a broken line,  $F = 1500$  N is a solid line, and  $F = 2000$  N is a dash-dot line. Each of these lines represents the frictional vibration limit for its respective clamp load values. Frictional vibrations occur below the line, and the system is vibration-free above it. The frictional vibration area for clamp load  $F = 1500$  N is shaded.

Figure 6 shows that the frictional vibration area is determined by the three variables: the damping value, the gradient of the friction coefficient and the clamp load.

In general, the following holds true:

For positive gradients of the friction coefficient, that is, when  $\mu' > 0$ , frictional vibrations never occur. For negative gradients of the friction coefficient, that is, when  $\mu' < 0$ , frictional vibrations occur in a sector that increases as the clamp load increases.



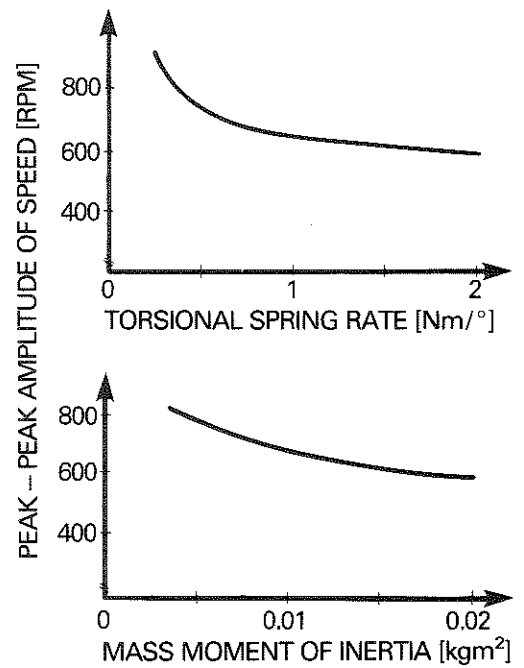
**Figure 6:** Friction vibration range as a function of damping, clamp load, and the gradient of the friction coefficient

Figure 7 shows the influence of the torsional spring rate and the mass moment of inertia in the vibration system when the gradient of the friction coefficient and the damping value are assumed to be constant.

The peak-to-peak amplitude of speed decreases only slightly both with an increasing torsional spring rate, as shown in the upper graph, but also with an increasing inertia, as shown in the bottom graph. Consequently, we can hardly expect to achieve noticeable improvement in chatter performance by changing the torsional spring rate and the mass moment of inertia.

Up till now, vibration calculations have treated the clamp load as a constant, thus ruling it out as a possible source of excitation.





**Figure 7:**  
Speed amplitude as a function of torsional spring rate and the mass moment of inertia

$$\mu' = -10 \cdot 10^{-3} \text{ s/m}; R = 0.1 \text{ Nms}$$

The following example shows that even when the curve for the friction coefficient is constant ( $\mu' = 0$ ), frictional vibrations are possible. For instance, if a non-parallel clutch disc is paired with a non-parallel clutch pressure plate, the resulting clamp load pulses at a frequency that corresponds to the speed differential between the engine and the transmission.

Figure 8 shows the influence on the peak-to-peak amplitude of speed with respect to the difference between the engine and transmission speeds. This graph was calculated based on a clamp load of 1500 N, subject to periodic change of  $\pm 5\%$ .

At the differential speed, which corresponds to the resonance speed of the drive train, speed vibrations occur. Their magnitude depends on the damping value, and they diminish rapidly on either side of the resonance speed.

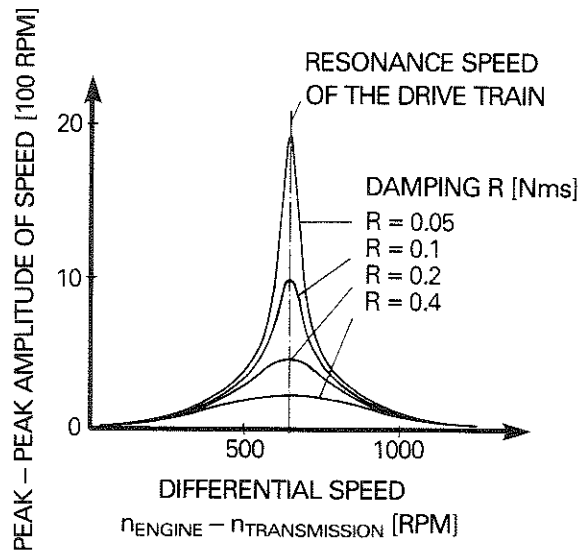


**Figure 8:**  
Torsional vibrations excited by clamp load fluctuations

Frictional vibrations that are caused in this way occur at precisely defined speed differentials between the engine and the transmission. Consequently, it is easy to pinpoint this cause by measuring vibrations in the vehicle.

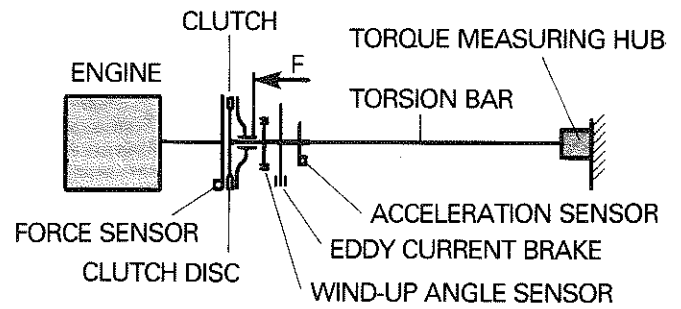
### Chatter Test Stand for Determining the Gradient of the Friction Coefficient

Test stands that are currently in use for the purpose of facing development are not appropriate for representing the high, speed-related fluctuations that occur at frequencies of approximately 10 Hz in conjunction with chatter. Furthermore, only forced vibrations are possible, as opposed to self-induced vibrations. Therefore, these test stands are inappropriate for determining the gradient of the friction coefficient.

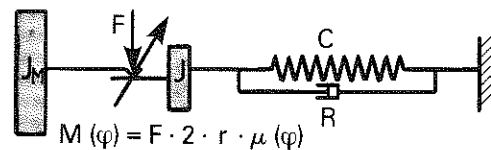
In order to study friction vibrations and specifically to determine the gradient of the friction coefficient, LuK has developed a new test stand.

Figure 9 shows a block diagram of this test stand, the vibration model, and the related differential equation.

## FRICTIONAL VIBRATION TEST STAND



### VIBRATION MODEL



**Figure 9:**  
Frictional vibration test stand and vibration model

$$J \cdot \ddot{\varphi} + R \cdot \dot{\varphi} + C \cdot \varphi = M(\varphi) = F \cdot 2 \cdot r \cdot \mu(\varphi)$$

The clutch is driven by a controlled-speed electric motor. On the output side, the clutch disc is attached to one end of a long torsion bar, which simulates the torsionally elastic drive train. Sensors are attached to the torsion bar to measure torsional movement in terms of the torsion angle and acceleration. An eddy-current brake allows the introduction of a speed-proportional damping value. The other end of the torsion bar is rigidly clamped in a torque measuring hub. The adjustable clutch clamp load is determined using load sensors.

The torsional spring rate  $C$  of the torsion bar corresponds roughly to that of the drive train for a compact passenger car. The inertia  $J$  includes the clutch disc and the transmission.

Figure 10 shows typical test results with a chattering facing for a drive speed of 500 rpm. The clutch disc vibrates with an amplitude of 500 rpm and always achieves the engine speed in short static friction phases.

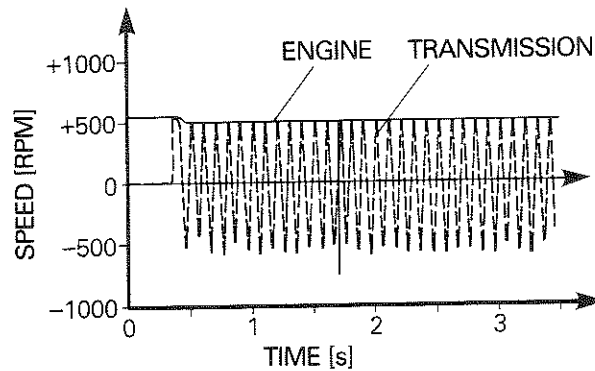


**Figure 10:**  
Speed curve during chatter

The top graph in Figure 11 shows a schematic section of this measurement. Below this graph, we see a synchronous curve for the differential speed. Using the measured curves for the torsion angle and clutch disc acceleration, it is possible to calculate the clutch torque at each point in time by means of the differential equation and to determine the curve of the friction coefficient with respect to time, as plotted in the bottom graph. The friction coefficient pulses periodically with the frequency of the frictional vibrations and is always at its maximum in conjunction with the minimum slip speed and vice versa.

Figure 12 shows the friction coefficient as a function of the slip speed for one period. The curve is almost identical for both increasing and decreasing slip speed. In this example, the friction coefficient decreases in inverse proportion to the slip speed.

The friction coefficient curve yields a gradient of:

$$\mu' = \frac{\Delta \mu}{\Delta v} = \frac{\mu_2 - \mu_1}{v_2 - v_1} = \frac{0.37 - 0.43}{8 \text{ m/s} - 0 \text{ m/s}} = -7.5 \cdot 10^{-3} \text{ [s/m]}$$

During testing, as has already been clearly noted from Figure 10, recognizable amplitude fluctuations occur between the individual vibrations. They are probably attributable to minimal fluctuations in  $\mu'$ . In this test, the variation for  $\mu'$  lay between  $-8.5 \cdot 10^{-3} \text{ s/m}$  and  $-7 \cdot 10^{-3} \text{ s/m}$ . The gradient for the friction coefficient  $\mu'$  must therefore be determined based on the average value of several vibrations.

We used this procedure to calculate the gradient of the friction coefficient for standard production facings. The clamp load was constant at 1500 N, and we varied the temperature and the speed.

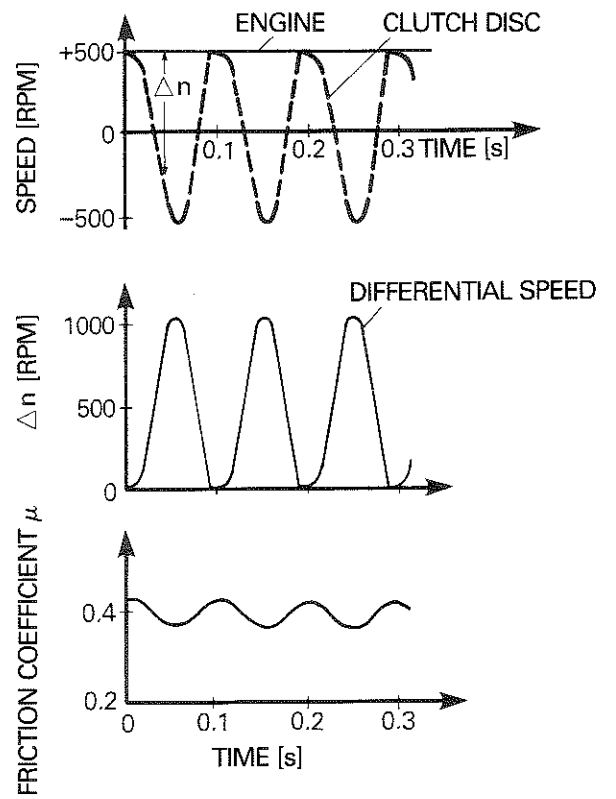
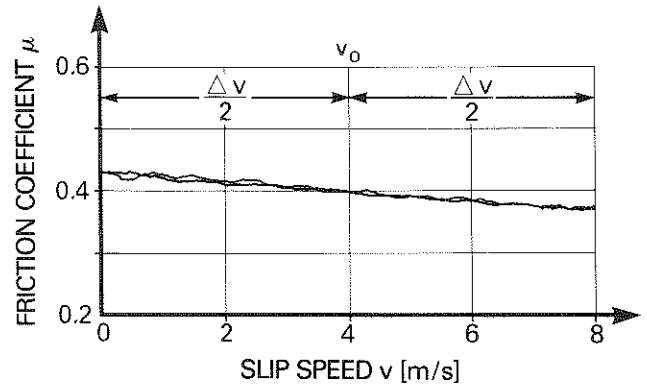


**Figure 11:**  
Speed, differential speed  
and friction coefficient in the  
friction vibration  
test



GRADIENT OF THE FRICTION COEFFICIENT

$$\mu' = \frac{\Delta \mu}{\Delta v} = \frac{\mu_2 - \mu_1}{v_2 - v_1} = \frac{0.37 - 0.43}{8 \text{ m/s} - 0 \text{ m/s}} = -7.5 \cdot 10^{-3} \text{ [s/m]}$$

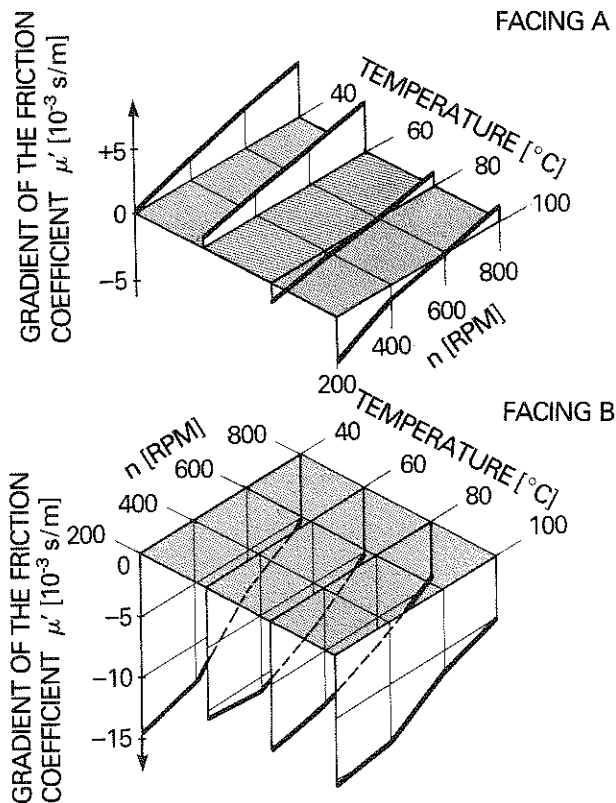
**Figure 12:** Friction coefficient curve and the gradient of the friction coefficient

Figure 13 shows the results for two facings. Facing A is a chatter-resistant material that has been used successfully to solve numerous problem cases, while Facing B is only applicable for vehicles that are not prone to chatter. Each graph shows the gradient of the friction coefficient  $\mu'$  for a temperature of 40°C, 60°C, 80°C and 100°C as a function of the speed, which varies from 200 rpm to 800 rpm.

Comparison of the two graphs shows the very high difference in the gradient of the friction coefficients for both facings with very low  $\mu'$  values for Facing B in comparison to Facing A.

As can be seen in the top graph, the gradient of the friction coefficient  $\mu'$  for facing A increases with increasing speed and decreases a little when the temperature increases. In the lower temperature range, the  $\mu'$  values are positive. Only higher temperatures, starting at about 80°C, and low differential speeds yield negative, that is, decreasing friction coefficients.

Facing B produces only negative gradients of the friction coefficient, which increase as a function of both speed and temperature.



**Figure 13:**  
Gradient of the friction coefficient  $\mu'$  comparison of facing A with facing B

Previous tests to determine the gradients of the friction coefficient have encompassed a limited speed and temperature range and need to be expanded to include the entire stress spectrum. However, currently existing values for the gradient of the friction coefficient present excellent possibilities for evaluating the chatter performance of friction materials.

If we compare the values determined for  $\mu'$  with Figure 6, we can see that the drive train for Facing A is free of frictional vibrations starting from a damping value of about 0.1 Nms, while frictional vibrations occur with Facing B up to a damping value of about 0.4 Nms. According to our measurements, drive train damping in the passenger car tested lay between about 0.1 and 0.5 Nms. Thus Facing A is chatter-free. This corresponds to our practical experience.

Because most clutch facings are hygroscopic and impregnation with sodium nitrite ( $\text{NaNO}_2$ ) makes this problem worse, we studied the effect of humidity on chatter.

In the case of wet, non-impregnated facings, the gradient for the friction coefficient falls to  $\mu' = \text{about } -20 \cdot 10^{-3} \text{ s/m}$ , but it rises to a normal level again after a few seconds because the facings dry out rapidly due to frictional heat. In the case of facings with sodium nitrite impregnation, the gradient of the friction coefficient decreases to about the same value as without impregnation, but increases then much more slowly. Possibly more moisture is bonded in the form of water of crystallization due to the sodium nitrite. This water is only given off very slowly and in conjunction with considerably higher temperatures. Consequently, we should avoid impregnation with sodium nitrite if at all possible.

## Summary

Based on theoretical studies, the basic principles governing frictional vibrations have been presented with respect to

- the gradient of the friction coefficient
- the damping value
- the clamp load
- the mass moment of inertia and
- the torsional spring rate of the drive train.

The discussion has revealed that frictional vibrations occur essentially in the presence of low drive train damping values and a negative gradient of the friction coefficient. Clamp load has a smaller effect. Other parameters studied have hardly any effect on chatter. Because of the good efficiency required and other comfort aspects, drive train damping cannot be increased significantly.

Consequently, our primary goal should be to develop friction materials with positive gradients of the friction coefficient.

The "chatter test stand" introduced here provides a simple means for determining the gradient of the friction coefficient, which is essential for chatter. Curves for the gradient of friction coefficient can be quickly found and used for optimizing facing materials.

If this option is fully exploited, it is possible to develop facings specifically for positive gradients of the friction coefficient without having to resort to otherwise time-consuming in-vehicle chatter tests.

Hence this development represents a way to overcome in-vehicle clutch chatter.

#### **Bibliography**

- [1] Newcombe, T. P. and Spurr, R. T.  
Clutch Judder, International Automobile Congress of FISITA 1972, 1/16
- [2] Jarvis, R. P. and Oldershaw, R.M.  
Clutch Judder in Automobile Drivelines, Proc Instn Mech Engrs 1973, Vol 187 27/73
- [3] Krause, R.  
Selbsterregte Reibschwingungen bei Kupplungslamellen [Self-induced Frictional Vibrations in Clutch Plates], Dissertation, Karlsruhe 1965